In-flight Simulation of an Aircraft Using Linear Quadratic Gaussian Controller

Seyyed Javad Mohammadi Baygi

Islamic Azad University, Damghan Branch, Damghan, Iran

ABSTRACT: The in-flight simulator is one of the various kinds of aircraft simulators at which a real aircraft provides a platform for simulating the dynamic responses of another aircraft. In this paper, the capability of the in-flight simulation of an aircraft by a host aircraft simulator using the linear quadratic gaussian (LQG) controller is presented. Initially, the maximum likelihood algorithm and the flight test data are used to estimate the aerodynamic derivatives of the guest aircraft and consequently drive its high-order aerodynamic model. Then, the linear and nonlinear models of both aircraft in the longitudinal and lateral modes are constructed and the proper LQG controllers are designed for the in-flight simulation of the guest aircraft responses caused by the host aircraft simulator. Next, by applying different commands to the control surfaces of the guest aircraft, its linear and nonlinear dynamic responses are simulated in the longitudinal and lateral modes. Finally, the simulated flight profiles of the guest aircraft are tracked by the host aircraft simulator in the linear and nonlinear schemes. To validate the capability of the LQG controllers for tracking the guest aircraft response, the flight test profile of the guest aircraft is also simulated by the host aircraft simulator.

1- INTRODUCTION

Nowadays, according to their capabilities and applications, different types of flight simulators are developed. In this regard, achieving a higher fidelity in the aircraft simulation response is one of the most important issues in the flight simulator research, which are followed by the evolution of the ground-based simulators in the motion, vision, and washout systems.

In-flight simulators are also known as a type of flight simulators that without having the limitations of the ground-based simulators, a real aircraft is used as a real platform for simulating many other aircraft responses and/or unusual conditions. In other words, a real aircraft, named as the host aircraft, simulates another aircraft response, named as the guest aircraft. For example, during the test pilot training, a real flight condition could be presented for the pilot [1] and the emergency conditions could be simulated safely, as the safety pilot could switch the system off and resume the control of the host aircraft when problem occur [2].

Also, in-flight simulators provide a safe, low cost and reliable test-bed for new aircraft research and development, so that if the purpose is to upgrade the flight control system, engineers could experience the concepts that they have merely studied theoretically [3, 4]. For example, in-flight simulators were employed in the flight control systems investigations for the space shuttles and also they were used for pilot training

before the main missions [5].

In this respect, Fig. 1 shows a concept for the flight control system, which could be used in an in-flight simulator.

In this regard, the main applications of the in-flight simulation are as follows [7-12]:

· Development of a new aircraft
· Training the pilots
· Advanced control development for piloted aircraft or UAVs
· Safe test bed for research and development for new technology
· Airborne system integration test
· Handling quality/flight control research
· Upset recovery training

The concept of in-flight simulation is based on controlling the host aircraft response by a controller that could simulate the response of the guest aircraft and track its flight profile.

In general applications, there are two groups of in-flight simulators [6]:

· Dynamic in-flight simulators
· In-flight simulators of the aircraft performance

In the dynamic in-flight simulators, the computers completely control the host aircraft response, change the host aircraft dynamics, and force it to fly as another aircraft. In-flight simulators of the guest aircraft performance are much simpler. They can be used as a support aircraft and sent for the duty when deemed necessary.
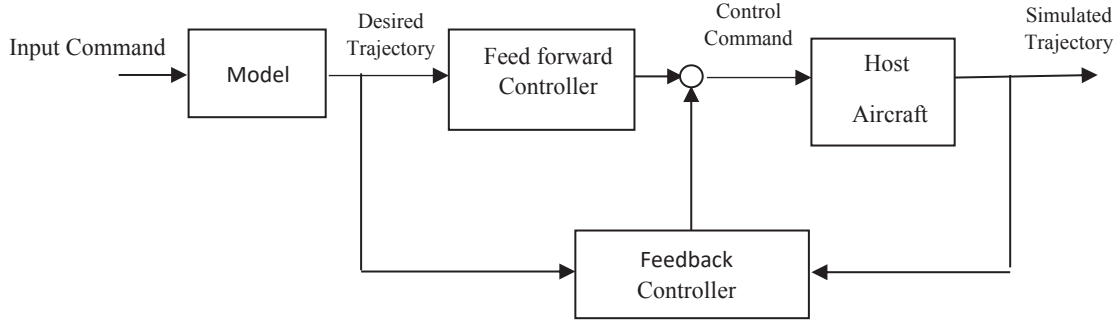
*Corresponding author's email: Mohammadi.s.j@gmail.com

Fig. 1. A concept for the flight control system in an in-flight simulator

The most important users of the inflight simulators in the United State are the United State air force, Navy, and Army, as well as NASA, FAA, test pilot schools and many aircraft manufacturers. Accordingly, several reports have been written on the different in-flight simulation purposes that use the dissimilar aircraft as simulators. Shafer [6] presented a brief history of in-flight simulators at the NASA's Dryden Flight Research Center where several in-flight simulators have been employed such as F-100C, NT-33A, F-8, F-102A, F-104, and F5D. Investigations on the approach and landing F-104 using new techniques, developing control systems in the X-15, researches on the approach and landing of X-15, simulation of a supersonic aircraft response and a hypersonic glider response, test pilots training, studies on the flight path control using throttles only, etc. are some typical works at Dryden Flight Research Center [6, 12].

Calspan's flight research division is also another corporation that uses the in-flight simulators for training the pilots and evolution of the flight control systems. Weingarten [13] discusses the development of in-flight simulators in the Calspan Corporation. In this sense, Calspan has used different in-flight simulators for airborne research and development of several flight control systems.

Kim [14] proposed the utilization of in-flight simulators as proper evaluation methods such that the designed flight control law can be verified in a real flight condition.

Fernandes [15] proposed a PID controller for the trajectory following of a micro quad-rotor platform. Pashilkar [16] presented a review of developments in the flight simulation since its inception and described the latest trends in the use of modeling and simulation for the design of flying vehicles. Mohammadi [17] designed a tracking controller for the in-flight simulation of fighter aircraft by an unmanned aerial vehicle (UAV) platform.

Watson [18] described the process of in-flight simulation for the NASA/Army variable stability helicopter CH-47B to investigate the handling quality effects of the pitch-roll cross-coupling characteristics of single-main-rotor helicopters. Thus, the comparison of the in-flight simulation model with the actual aircraft responses has been accomplished to demonstrate the fidelity of the in-flight simulation process. Chehadeh [19] also designed a rule for in-flight tuning of PID controllers for UAV.

In this research, the dynamic simulation of a guest aircraft response using a linear quadratic gaussian (LQG) controller in a host aircraft platform is presented. First, the mathematical model of an aircraft and the brief descriptions of the LQG controllers are discussed. Then, the maximum likelihood algorithm is employed to estimate the aerodynamic derivatives of the guest aircraft from its flight test data. The aerodynamic, geometric, propulsive and mass characteristics of two aircraft are used to establish the mathematical dynamic models of the host and guest aircraft. Then, the required controllers for the in-flight simulation of the guest aircraft responses in the longitudinal and lateral modes are designed. Using the designed LQG controllers and applying different commands to the control surfaces of the guest aircraft, its linear and nonlinear dynamic responses are simulated by the host aircraft simulator. Finally, the flight test profile of the guest aircraft is tracked and simulated by the host aircraft simulator, as well.

2- MATERIAL AND METHODS
2.1 Aircraft mathematical model

It is assumed that a standard rigid-body model is governing the aircraft dynamics. The nonlinear mathematical model of aircraft consists of six dynamic equations, three rotational kinematic and three navigational equations. The mathematical model that is fully described previously in the references [20], [21] and [23] is expressible as follows:

Six dynamic equations:

$$\dot{u} = g.\sin\Theta + v.r - w.q + \frac{\overline{q}.S.C_x + T}{M}$$

$$\dot{v} = g.\cos\Theta.\sin\Phi + w.p - r.u + \frac{\overline{q}.S.C_y}{M} \qquad (1)$$

$$\dot{w} = g.\cos\Theta.\cos\Phi + u.q - v.p + \frac{\overline{q}.S.C_z}{M}$$

$$I_{xx}\dot{p} - I_{xy}\dot{r} = \overline{q}.S.b.C_l + (I_{yy} - I_{zz}).r.q + I_{xz}.p.q$$

$$I_{zz}\dot{r} - I_{xz}\dot{p} = \overline{q}.S.b.C_n + (I_{xx} - I_{yy}).p.q + I_{xz}.qr \qquad (2)$$

$$I_{yy}\dot{q} = \overline{q}.S.c.C_m + (I_{zz} - I_{xx}).p.r + I_{xz}.(r^2 - p^2)$$

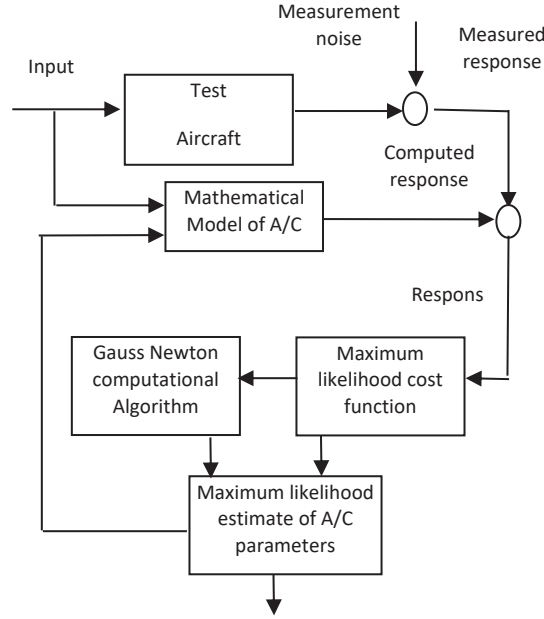**Fig. 2. Maximum likelihood concept [24]**

Three kinematic equations:

$$\dot{\Phi} = p + \tan\Theta.(q.\sin\Phi + r.\cos\Phi)$$
$$\dot{\Theta} = q.\cos\Phi - r.\sin\Phi$$
$$\dot{\Psi} = \frac{q.\sin\Phi + r.\cos\Phi}{\cos\Theta}$$

(3)

Three navigational equations:

$$\dot{x}_E = u.\cos\Theta.\cos\Psi + v.(\sin\Phi.\sin\Theta.\cos\Psi - \cos\Phi.\sin\Psi) + $$
$$w.(\cos\Phi.\sin\Theta.\cos\Psi + \sin\Phi.\sin\Psi)$$
$$\dot{y}_E = u.\cos\Theta.\sin\Psi + v.(\sin\Phi.\sin\Theta.\sin\Psi + \cos\Phi.\cos\Psi) + $$
$$w.(\cos\Phi.\sin\Theta.\sin\Psi - \sin\Phi.\cos\Psi)$$
$$\dot{h} = u.\sin\Theta - v.\sin\Phi.\cos\Theta - w.\cos\Phi.\cos\Theta$$

(4)

Where: $\bar{q} = \frac{1}{2}\rho V_t^2$ and all parameters of the model are fully described in Ref [20].

The dynamic model of an aircraft can be represented in a the general state-space form in which the state vector is:

$$x = [u \quad v \quad w \quad p \quad q \quad r \quad \phi \quad \theta \quad \psi]$$

(5)

and the control input vector is:

$$u = [\delta_e \quad \delta_{th} \quad \delta_a \quad \delta_r]^T$$

(6)

where:

$$\dot{x} = f(x,u)$$

(7)

which this nonlinear model presents a set of coupled

nonlinear ordinary differential equations. The output equations can be modeled as follows:

$$y = h(x,u)$$

(8)

2.2 Brief Description of Maximum Likelihood Estimation Method

Considering the general case of the aircraft model as follow:

$$x(t_0) = x_0$$
$$\dot{x}(t) = Ax(t) + Bu(t)$$
$$z(t_i) = cx(t_i) + Du(t_i) + G\eta_i$$

(9)

Where x is the state vector, z is the observation vector, u the control vector, and the defined stability and control derivatives in Eq. (1) and (2) are contained primarily in the matrices A and B.

In this respect, Fig. 2 shows the concept of maximum likelihood algorithm in which a full description of this method is presented by Maine and Iliff [24] and other researchers previously [25-27]. At this method, the measured response of the aircraft is compared with the estimated response, and the difference between these responses is called as the response error of the aircraft.

Then, the Gauss-Newton computational algorithm is used to find the coefficient values that optimizes the likelihood functional. Equation 10 represents the cost function of the maximum likelihood estimator algorithm [24]:

$$J(\xi) = \frac{1}{2}\sum_{i=1}^{n}[z(t_i) - \tilde{z}_\xi(t_i)]^T (GG^T)^{-1}[z(t_i) - \tilde{z}_\xi(t_i)]$$
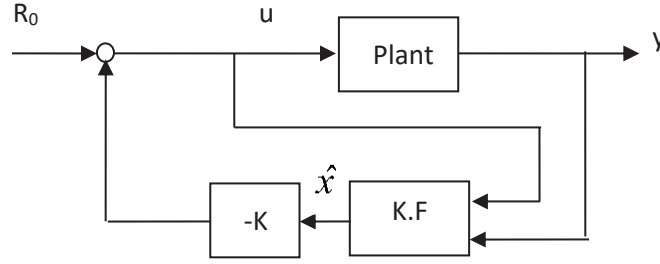
(10)

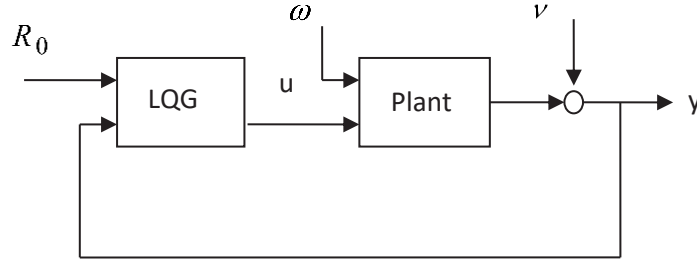**Fig. 3. The concept of the LQG controller [28]**

Fig. 4. Standard form of the LQG tracker [28]

Where, GG^T is the measurement noise covariance matrix and $\tilde{z}_\zeta(t_i)$ is the computed response estimate of z at the time t_i for a given value of the unknown parameter vector ζ as follows:

$$\xi = \{C_{L_0} \; C_{L_\alpha} \quad C_{L_\beta} \quad C_{L_{\alpha\beta}} \quad C_{L_{\alpha^2}}$$
$$C_{L_{\alpha^2\beta}} \quad C_{L_{\alpha^3}} \; C_{L_{\alpha^2\beta}} \quad C_{L_q} \quad C_{L_{q\alpha}} \quad ...\} \tag{11}$$

The cost function is a function of the difference between the measured and computed time histories.

To minimize the cost function $J(\zeta)$, the Newton-Raphson algorithm is applied, which chooses a successive estimates of the vector of unknown coefficients ζ. Let L be the iteration number, then $L+1$ estimate of $\hat\zeta$ is then obtained from the L estimate as:

$$\hat{\xi}_{L+1} = \hat{\xi}_L - [\nabla_\xi^2 J(\hat{\xi}_L)]^{-1}[\nabla_\xi^T J(\hat{\xi}_L)] \tag{12}$$

Where the first gradient can be defined as:

$$\nabla_\xi J(\xi) = -\sum_{i=1}^{N}[[z(t_i) - \tilde{z}_\xi(t_i)]^T (GG^T)^{-1}[\nabla_\xi \tilde{z}_\xi(t_i)]] \tag{13}$$

And the gauss-Newton approximation to the second gradient is:

$$\nabla^2_\xi J(\xi) = -\sum_{i=1}^{N}[\nabla_\xi \tilde{z}_\xi(t_i)]^T (GG^T)^{-1}[\nabla_\xi \tilde{z}_\xi(t_i)] \tag{14}$$

Each iteration of this algorithm provides a revised estimates of the unknown coefficients based on the response error. These revised estimates of the coefficients are then used to update the mathematical model of the aircraft, providing a revised estimated response and therefore a revised response error. Then the mathematical model is updated iteratively until a convergence criterion is satisfied. [24]

2.3 Application of LQG method

If the cost function of an optimal controller can be written as a quadratic function of the state and control vectors, then the controller can be defined as a linear quadratic regulator (LQR). This controller requires the full state feedback of the system, however during the practical applications, the full state feedback cannot be achieved and a state estimation process is required. In this regard, the LQG is assigned to the problem, which employs the Kalman filter as an estimator in the LQR problem.

In other words, in the LQG problem, the Kalman filter estimates the state of the system and then an optimal controller is designed using the estimated state.

Fig. 3 shows the concept of the LQG controller as follows:

The LQG tracker or the LQG servo controller is defined as a controller with a nonzero reference command R_0, for which a certain reference command should be tracked and the compensators ensure that the output of the system tracks the intended reference command such that the measurement noise v and process disturbances w are rejected. Therefore, the standard form of the LQG tracker can be considered as is shown in Fig. 4:

Knowing that the state-space representation of a system can be written as follows:

$$\dot{x} = Ax + Bu + \omega$$
$$y = Cx + Du + \upsilon \tag{15}$$

with X the state, u the input, y the output, and A, B,

C, and D the system matrices, parameters υ and ω stand for the measurement and process noises, respectively. In addition, we have:

$$E\left\{\begin{bmatrix} \omega \\ \nu \end{bmatrix}\begin{bmatrix} \omega^T & \nu^T \end{bmatrix}\right\} = Q_{WV} = \begin{bmatrix} Q_{11} & Q_{12} \\ Q_{21} & Q_{22} \end{bmatrix}$$

$$Q_{11} = E\left[\omega\omega^T\right] \quad Q_{12} = E\left[\omega\nu^T\right] \tag{16}$$

$$Q_{21} = E\left[\nu\omega^T\right] \quad Q_{22} = E\left[\nu\nu^T\right]$$

For simplicity, it is assumed that ν and ω are independent. Hence Q_{12} and Q_{21} are both zero and

$$E[\omega\omega^T] \simeq N(0,Q)$$
$$E[\nu\nu^T] \simeq N(0,\mathrm{R}) \tag{17}$$

in which Q and R demonstrate the covariance matrices and N is zero-mean normally distributed random variable with covariance's of Q or R.

If the system is controllable and observable, the LQR control law is found by the minimization of the following cost function [28-30]:

$$\min J = E\{\int_0^\infty \begin{bmatrix} x^T & u^T \end{bmatrix} Q_{xu} \begin{bmatrix} x \\ u \end{bmatrix} dt\} \tag{18}$$

and due to the stochastic nature of the state variables, the minimization of the cost function expected value is required as follows:

$$\min J = E\{\int_0^\infty [\mathrm{x}^T(t)Q_1(t)\mathrm{x}(t) + \mathrm{u}^T(t)Q_2(t)\mathrm{u}(t)]dt\} \tag{19}$$

where $Q_1(t)$ is the state weighting matrix that is a symmetric positive semi-definite, and $Q_2(t)$ is the control-weighting matrix that is a symmetric positive definite, respectively.

In addition, the tracking error, which is the difference of R_0 and y, should be minimized in the LQG tracker.

$$\dot{e}_i = R_0 - y \tag{20}$$

in which, e_i is the tracking error function.

Thus, the cost function could be formulated as follows:

$$\min J = E\{\int_0^\infty (\begin{bmatrix} x^T & u^T \end{bmatrix} Q_{xu} \begin{bmatrix} x \\ u \end{bmatrix} dt + \mathrm{e}_i^T Q_i \mathrm{e}_i) dt\} \tag{21}$$

where, the above equation can be rewritten in the simple form:

$$\min J = E\{\int_0^\infty [\mathrm{x}^T(t)Q_1(t)\mathrm{x}(t) + \mathrm{u}^T(t)Q_2(t)\mathrm{u}(t) + \mathrm{e}_i^T Q_i \mathrm{e}_i]dt\} \tag{22}$$

$$e_i = \int_0^t (\mathrm{R}_0 - y) dt \tag{23}$$

In this regard, the optimal feedback controller could be found by numerical solution of the matrix Riccati differential equation, which is fully discussed by Skogestad [28].

In the LQR, the whole state is assumed to be available for the control at all the times and the noise is omitted in the analysis, but it is unrealistic. The extended Kalman filter, as an optimal observer, estimates the state variables contaminated by Gaussian white noise with specific variance.

The estimated $\hat{x}(t)$ can be calculated by the integration of the following ordinary differential equation [28-30]:

$$\dot{\hat{x}} = A\hat{x} + Bu + L(\mathrm{y} - C\hat{x}) \tag{24}$$

With an offline calculation of the following matrices:

$$L = PC^T R^{-1}$$
$$0 = AP + PA^T - PC^T R^{-1}CP + Q, \qquad 0 \le P \tag{25}$$
$$Q = E[\omega\omega^T], \qquad R = E[\nu\nu^T]$$

and by minimization of the following functional, the Riccati equation will be in the origin:

$$J[\hat{x}(\bullet)] = \int_{-\infty}^0 [(\hat{x} - \mathrm{x})(\hat{x} - \mathrm{x})^T]dt \tag{26}$$

3- CALCULATIONS AND APPLICATIONS OF THE METHODS

3.1 Identification of aerodynamic characteristics of the guest aircraft

A flight test has been conducted for investigation on the model of the guest aircraft and in-flight simulation capability of the host aircraft simulator. In this regard, the necessary training is given to the test pilot to apply the necessary persistency excitation on the aircraft control surfaces to stimulate the aircraft flight modes. Simultaneously the calibration of the sensors and the measuring instruments was checked and thereafter the flight test was performed. Then, the raw flight test information is gathered from the recording instruments and aircraft black box, in accordance with the flight data gathering protocol. Finally, the actual flight test data is extracted from the raw data by using the decoding formulas, which were presented for the aircraft flight test.

Fig. 5 shows a portion of the sample flight test data for the guest aircraft.

By using the maximum likelihood algorithm, the aerodynamic characteristics of the guest aircraft are estimated. The proposed estimated model for the aerodynamic functions of the guest aircraft is expressible as follows:

$$C_x = a_0 + a_1\alpha + a_2\dot{\alpha} + a_3\delta_h + a_4\tilde{q} + a_5\alpha\tilde{q}$$
$$C_y = b_0 + b_1\beta + b_2\delta_a + b_3\delta_r + b_4\tilde{p} + b_5\tilde{r} + b_6\beta\tilde{r} + b_7\beta\tilde{p}$$
$$C_z = e_0 + e_1\alpha + e_2\dot{\alpha} + e_3\delta_h + e_4\tilde{q} + e_5\alpha\tilde{q}$$
$$C_l = f_0 + f_1\beta + f_2\alpha\beta + f_3\beta^2 + f_4\tilde{p} + f_5\alpha\tilde{p} + f_6\tilde{r} + f_7\alpha\tilde{r} + f_8\delta_a + f_9\delta_r$$
$$C_m = g_0 + g_1\alpha + g_2\dot{\alpha} + g_3\delta_h + g_4\tilde{q} + g_5\alpha\tilde{q} \tag{27}$$
$$C_n = h_0 + h_1\beta + h_2\alpha\beta + h_3\beta^2 + h_4\tilde{p} + h_5\alpha\tilde{p} + h_6\tilde{r} + h_7\alpha\tilde{r} + h_8\delta_a + h_9\delta_r$$
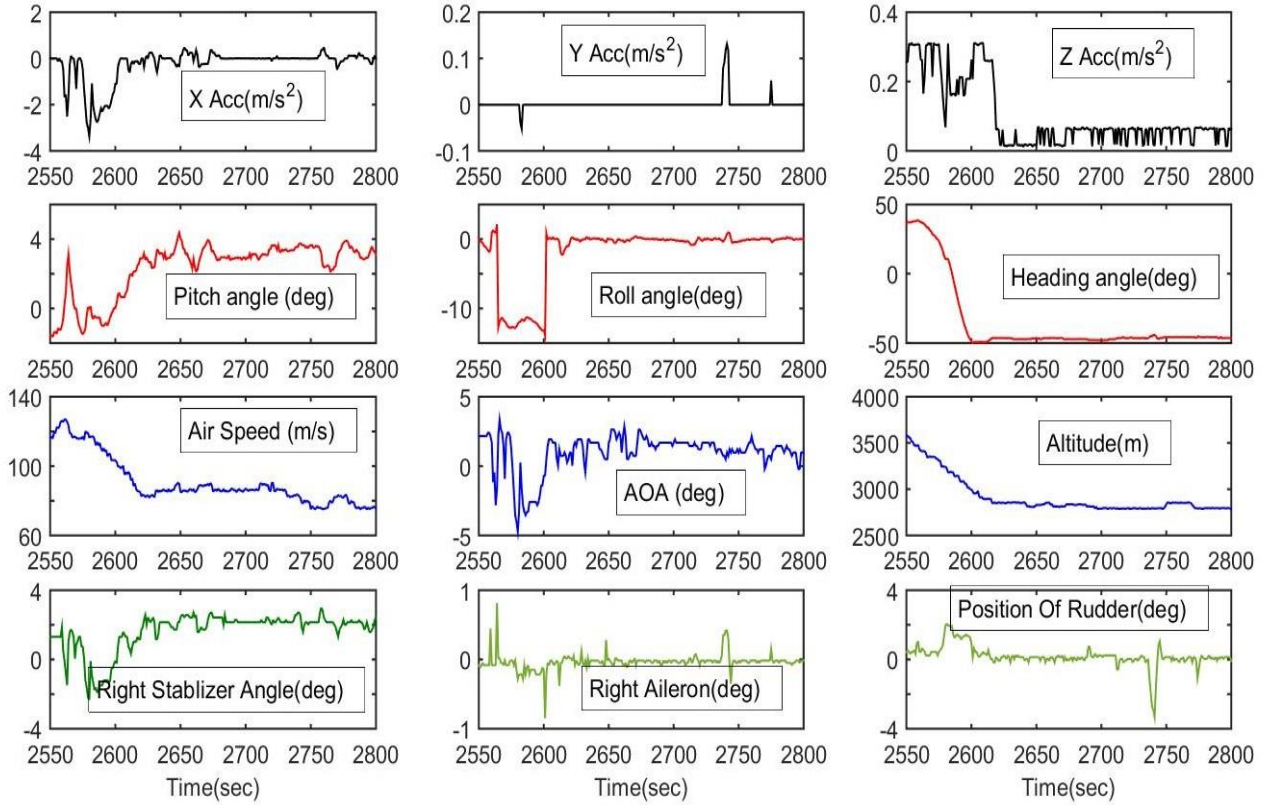
Fig. 5. A sample flight test data for the guest aircraft

Where:

$$\tilde{p} = pb/2V \qquad \tilde{q} = qc/2V \qquad \tilde{r} = rb/2V \qquad (28)$$

In this research, stands for the vector of unknown parameters and is defined as the vector of aerodynamic characteristics of the guest aircraft, which is estimated using the maximum likelihood algorithm [24].

$$\xi = \{a_0 \quad a_1 \quad a_2 \quad a_3 \quad a_4 \quad a_5 \\ b_0 \quad b_1 \quad b_2 \quad b_3 \quad b_4 \quad b_5 \quad b_6 \quad b_7 \quad ...\} \qquad (29)$$

Table 1 represents the estimation results of the maximum likelihood algorithm corresponding to the designed flight test of the guest aircraft.

The aerodynamic derivatives b6, b7, f3, f5, h3, and h5 play a negligible role in Equation 27 and as they might be submerged by the measurement errors and noises, they are set to zero and the identification process is being repeated sequentially.

3.2 Linearized dynamic models for the host/guest aircraft

In this research, a linearized model for the aircraft equations of motion [20 to 22] is used, such that:

$$E\dot{x} = Ax + Bu \qquad (30)$$

And

$$E = \begin{bmatrix} 1 & 0 & 0 & 0 \\ 0 & V - Z_{\dot{\alpha}} & 0 & 0 \\ 0 & 0 & 1 & 0 \\ 0 & M_{\dot{\alpha}} & 0 & 1 \end{bmatrix} ; B = \begin{bmatrix} X_{\delta h} & X_{\delta th} \cos\alpha \\ Z_{\delta h} & X_{\delta th} \sin\alpha \\ 0 & 0 \\ M_{\delta h} & M_{\delta th} \end{bmatrix} \quad (31)$$

$$A = \begin{bmatrix} X_u + X_{Tu}\cos\alpha & X_\alpha & -g\cos\gamma & 0 \\ Z_u - X_{Tu}\sin\alpha & Z_\alpha & -g\sin\gamma & V + Z_q \\ 0 & 0 & 0 & 1 \\ M_u + M_{Tu} & M_\alpha & 0 & M_q \end{bmatrix}$$

where all the parameters in Equation 31 are fully described in the references [20-22]. Parameter x is the state vector of the linear longitudinal dynamic model of the aircraft as follows:

$$x = \begin{bmatrix} u' \\ \alpha' \\ q' \\ \theta' \end{bmatrix} \qquad (32)$$

where:

u' : The longitudinal velocity perturbation;
α' : Angle of attack perturbation;
q' : Pitch rate perturbation;

Table 1. Aerodynamic coefficients for the high-order aircraft model

a0	2.54811e-2	b6	0	f4	-1.64813e-1	h0	0
a1	1.13654e-1	b7	0	F5	0	h1	4.88413e-2
a2	1.24011e-3	e0	0.27204e0	F6	8.82291e-2	h2	-2.21201e-2
a3	-4.15004e-2	e1	2.20125e0	f7	2.22081e-3	h3	0
a4	-2.33875e-3	e2	1.24099e-3	F8	1.81023e-1	h4	-3.10788e-2
a5	-1.17495e-3	e3	3.94080e-1	F9	1.47007e-2	h5	0
b0	0	e4	4.81599	g0	2.02937e-2	h6	-9.98471e-2
b1	-4.02735e-1	e5	4.22811e-2	g1	-8.66702e-2	h7	2.46700e-3
B2	-3.18042e-3	f0	0	g2	5.01853e-3	h8	-5.66427e-2
b3	1.24581e-1	f1	-1.8538e-1	g3	-1.37886e0	h9	-6.88025e-2
b4	-1.02506e-2	f2	-5.42285e-2	g4	-8.013501e-1		
b5	1.62401e-1	f3	0	g5	-4.09277e-2		

θ' : Pitch angle perturbation;

δe : Elevator deflection angle;

The guest (jet) aircraft has a length of 17.38 m, a wing area of 38.00 m² and a weight of 11000 kg. The flight test was performed at the altitude range of 1800 to 3600 m with an average airspeed of 95 m/s.

The linear longitudinal dynamic model of the guest aircraft, using the estimated aerodynamic characteristics of the aircraft obtained by the maximum likelihood algorithm, is as follows:

$$\dot{x} = \begin{bmatrix} -0.0158 & 12.8134 & 0 & -32.1741 \\ -0.0003 & -0.588 & 0.9897 & -0.0024 \\ 0.0008 & -7.9844 & -1.9050 & 0.0018 \\ 0 & 0 & 1 & 0 \end{bmatrix} x$$
$$+ \begin{bmatrix} 0.0062 & 0.0115 \\ -0.1283 & 0.0002 \\ 0 & 0 \\ -30.7985 & 2.1207 \end{bmatrix} \begin{bmatrix} \delta_h \\ \delta_{th} \end{bmatrix} \tag{33}$$

where:

$$\dot{x} = E^{-1}Ax + E^{-1}Bu \tag{34}$$

According to references [20-22], the linear lateral dynamic model of the guest aircraft is used in which:

$$E = \begin{bmatrix} V & 0 & 0 & 0 \\ 0 & 1 & 0 & 0 \\ 0 & 0 & 1 & 0 \\ 0 & M_{\dot\alpha} & 0 & 1 \end{bmatrix} \quad ; B = \begin{bmatrix} Y_{\delta a} & Y_{\delta r} \\ 0 & 0 \\ L_{\delta a} & L_{\delta r} \\ N_{\delta a} & N_{\delta r} \end{bmatrix} \tag{35}$$

$$A = \begin{bmatrix} X_u + X_{Tu}\cos\alpha & X_\alpha & -g\cos\gamma & 0 \\ Z_u - X_{Tu}\sin\alpha & Z_\alpha & -g\sin\gamma & U+Z_q \\ 0 & 0 & 0 & 1 \\ M_u + M_{Tu} & M_\alpha & 0 & M_q \end{bmatrix}$$

where the references [20- 22] presents detailed descriptions of the parameters in Equation 35 and x is the state vector of the linear lateral dynamic model of the aircraft that is formulated as follows

$$x = \begin{bmatrix} \beta' \\ \phi' \\ p' \\ r' \end{bmatrix} \tag{36}$$

where:

β' : Sideslip angle perturbation;

ϕ' : Roll angle perturbation;

p' : Roll rate perturbation;

r' : Yaw rate perturbation;

δa : Ailerons deflection angle;

δr : Rudder deflection angle;

Therefore, for the lateral aerodynamic model of the guest aircraft, we have:

$$\dot{x} = \begin{bmatrix} -1584 & 0.0903 & 0.0002 & -0.9961 \\ 0 & 0 & 1.0000 & 0 \\ -4.4340 & 0 & -0.2762 & 0.1256 \\ 5.1768 & 0 & -0.0675 & -0.7855 \end{bmatrix} x$$
$$+ \begin{bmatrix} 0 & 0.0166 \\ 0 & 0 \\ 3.7943 & 0.3713 \\ -0.0384 & -3.3207 \end{bmatrix} \begin{bmatrix} \delta a \\ \delta r \end{bmatrix} \tag{37}$$

Similarly, the host (jet) aircraft, has the length of 5.51 m, wing area of 2.26 m², and a weight of 495 kg. Consequently, the linear longitudinal dynamic model of the host aircraft at the average airspeed of 95 m/s is calculated as follows:

$$\dot{x} = \begin{bmatrix} -0.0277 & 6.1556 & 0 & -9.8007 \\ 0.00017 & -1.5172 & 0.9873 & -0.0033 \\ 0.0112 & -37.0243 & -1.5220 & 0.0016 \\ 0 & 0 & 1.000 & 0 \end{bmatrix} x$$
$$+ \begin{bmatrix} 0.0012 & 0.0102 \\ -0.1484 & 0.0084 \\ 0 & 0 \\ -21.78 & 5.1820 \end{bmatrix} \begin{bmatrix} \delta e \\ \delta_{th} \end{bmatrix} \tag{38}$$
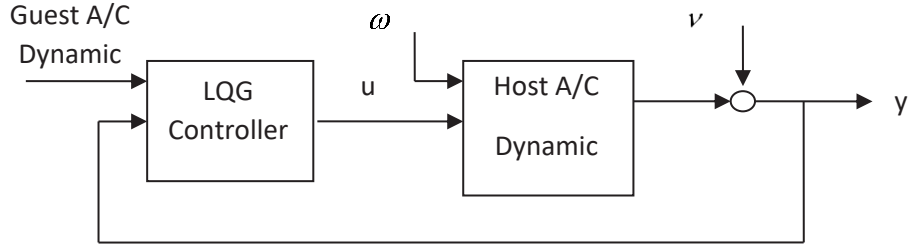
Fig. 6. The proper LQG controller for inflight simulation of the aircraft

In the same way, the linear lateral dynamic model of this aircraft is expressible as follows:

$$\dot{x} = \begin{bmatrix} -0.2776 & 0.0903 & -0.0058 & -0.9882 \\ 0 & 0 & 1.000 & 0 \\ -20.935 & 0 & -5.9123 & 1.371 \\ 4.371 & 0 & -0.280 & -0.8301 \end{bmatrix} x$$
$$+ \begin{bmatrix} 0 & 0.696 \\ 0 & 0 \\ 26.2292 & 0.932 \\ 1.7336 & -5.5559 \end{bmatrix} \begin{bmatrix} \delta a \\ \delta r \end{bmatrix} \tag{39}$$

3.3 The LQG servo controller gains for in-flight simulation of the guest aircraft

In this section, the LQG servo controllers are designed for the in-flight simulation of the guest aircraft responses using the longitudinal and lateral dynamic models of the host aircraft. These controllers are used to be applied in the host aircraft control system. The designed LQG servo controllers should control the host aircraft system and change its dynamic responses until it simulates the guest aircraft dynamic and tracks its flight profile.

In this regard, the guest aircraft dynamic response is considered as the reference command for the LQG controller that is shown in Fig. 3. Fig. 6 demonstrates the proper LQG controller for the in-flight simulation of the aircraft.

Accordingly, the Kalman filter gain in the longitudinal mode of the host aircraft is calculated as follows:

$$L = \begin{bmatrix} 2.4570 \\ 0.2229 \\ -0.3597 \\ -0.4404 \end{bmatrix} \tag{40}$$

For this reason, the Riccati equation at the longitudinal mode is solved, Hence we have:

$$P = \begin{bmatrix} 14.2345 & -0.0995 & 1.6488 & -1.7568 \\ -0.0995 & 0.4320 & -0.5091 & 0.3324 \\ 1.6488 & -0.5091 & 13.3740 & 0.4952 \\ -1.7568 & 0.3324 & 0.4952 & 1.0252 \end{bmatrix} \tag{41}$$

Similarly, in the lateral mode, these parameters are calculated as follows:

$$P = \begin{bmatrix} 0.9765 & 0.6647 & -2.4445 & 0.6754 \\ 0.6647 & 1.5452 & -0.7985 & -0.3903 \\ -2.4445 & -0.7985 & 8.2388 & -2.9725 \\ 0.6754 & -0.3903 & -2.9725 & 4.5010 \end{bmatrix} \tag{42}$$

$$L = \begin{bmatrix} -0.0791 \\ 0.4208 \\ -0.2936 \\ 0.1900 \end{bmatrix} \tag{43}$$

The controller gain that is intended to minimize the average of the LQR cost function in the longitudinal mode is also calculated as follows:

$$K = \begin{bmatrix} 6.7379 & 10.3765 & -0.8069 & -15.8589 & -14.1360 \\ 0.1143 & 0.1501 & -0.0082 & -0.2324 & -0.2947 \end{bmatrix} \tag{44}$$

where, in the lateral mode, this gain is obtained as:

$$K = \begin{bmatrix} 0.5302 & 1.0610 & 0.8778 & 0.9985 & -14.0393 \\ 0.1478 & -0.0912 & -0.0649 & -0.2756 & 1.2039 \end{bmatrix} \tag{45}$$

4- RESULTS AND DISCUSSION
4.1 In-flight simulation of the guest aircraft response by the host aircraft simulator

Using the designed LQG controllers for the host aircraft control system, the longitudinal and lateral dynamic responses of the guest aircraft are simulated by the host aircraft simulator. First, the in-flight simulation of the guest aircraft response is accomplished for the linear model and all of its flight profiles are tracked in the longitudinal and lateral modes by the host aircraft simulator, as well. Therefore, different commands are applied to the control surfaces of the guest aircraft, such as the elevator, rudder, and aileron. Figs.7 and 8 demonstrate two samples for the in-flight simulations in linear form of the guest aircraft responses in the longitudinal and lateral modes. It should be noticed that these results only demonstrate the perturbation parameters around the nominal points of the
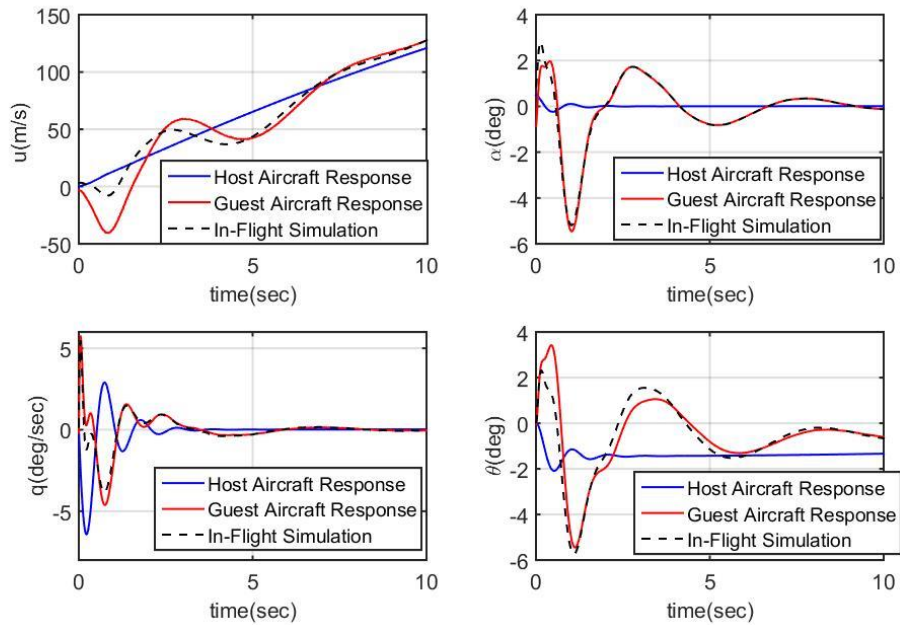
Fig. 7. A sample of linear in-flight simulation of the guest aircraft response in the longitudinal mode
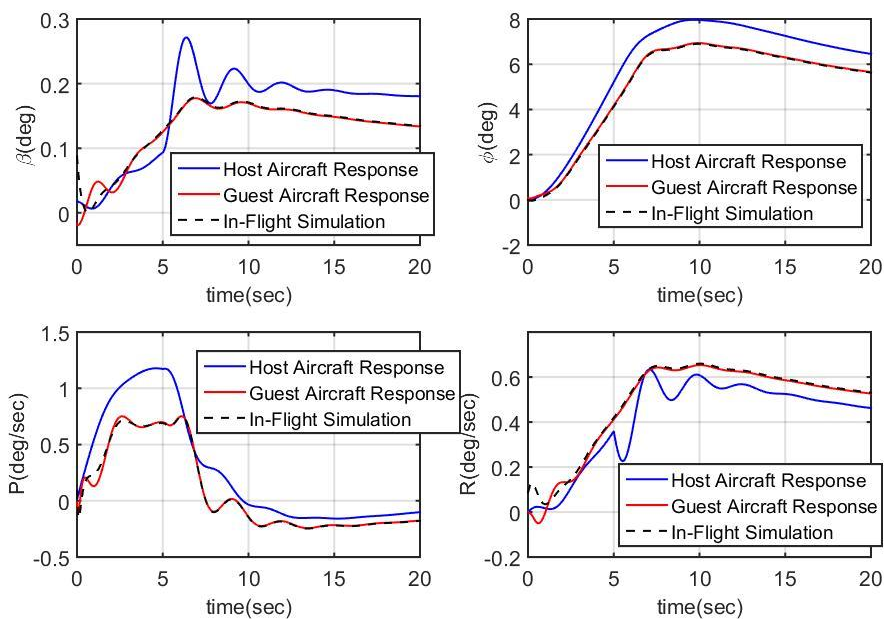

Fig. 8. A sample of linear in-flight simulation of the guest aircraft response in the lateral mode

flight path for the host and guest aircraft and they demonstrate the tracking accuracy of the guest aircraft flight profiles by the host aircraft simulator using liner analysis.

4.2 Application of the LQG controller for the nonlinear model of the host aircraft

In this section, the LQG controllers are used for in-flight simulation of the guest aircraft response by the host aircraft simulator assuming nonlinear models for both aircraft.

For this purpose, first, the control commands necessary to follow the dynamic behavior of the guest aircraft are extracted in both longitudinal and lateral modes via the linearized

model of the host aircraft Then, these designed commands are simultaneously applied to the nonlinear model of the host aircraft and the behavior of the host aircraft is simulated in a nonlinear scheme. finally, the tracking error of the guest aircraft behavior by the host aircraft is measured.

Fig. 9 illustrates the application concept of LQG controller on the host aircraft simulator model.

To this end, different commands are applied to the control surfaces of the guest aircraft and the host aircraft simulator simulates the guest aircraft nonlinear dynamic response using the derived commands from the linear model of the host aircraft simulator. Fig. 10 demonstrates a sample of the input
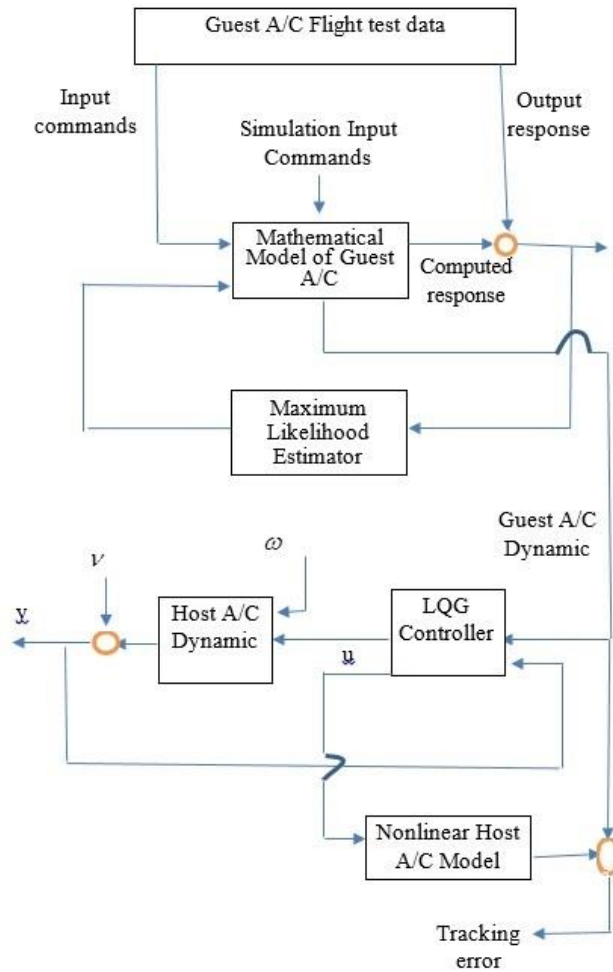
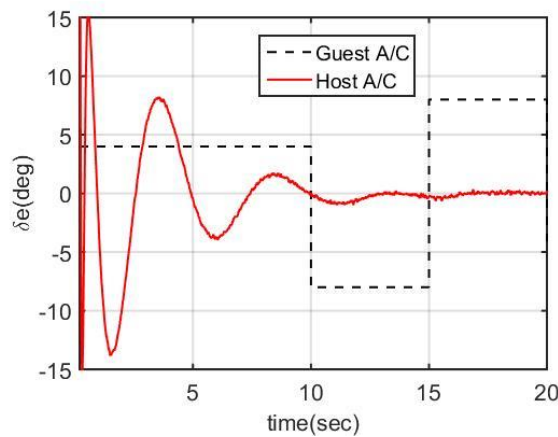**Fig. 9. The application concept of the LQG controller on the host aircraft simulator**

Fig. 10. A sample of elevator surface control input command for the guest aircraft against its equivalent control command for the host aircraft simulator

command to the elevator control surface of the guest aircraft and the equivalent control command for the host aircraft simulator, which is applied by the LQG controller. Fig. 11 shows the nonlinear in-flight simulations of the guest aircraft response by the host aircraft simulator in the longitudinal mode. For a further demonstration, Fig. 12 shows the tracking error of this in-flight simulation in the longitudinal mode.

Fig. 13 also demonstrates a sample of the aileron and rudder surface control inputs command for the guest aircraft against their equivalent control commands for the host aircraft. Fig. 14 shows the nonlinear in-flight simulations of the guest aircraft response by the host aircraft simulator in the lateral mode. Fig. 15 also shows the tracking error of the in-flight simulation of the guest aircraft in the lateral mode.
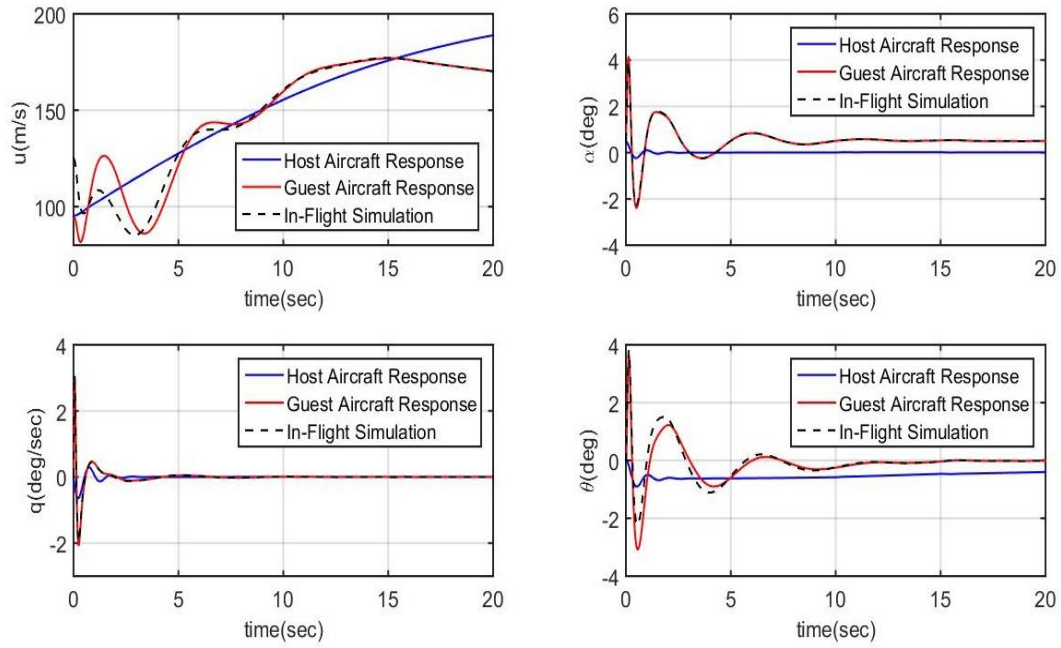
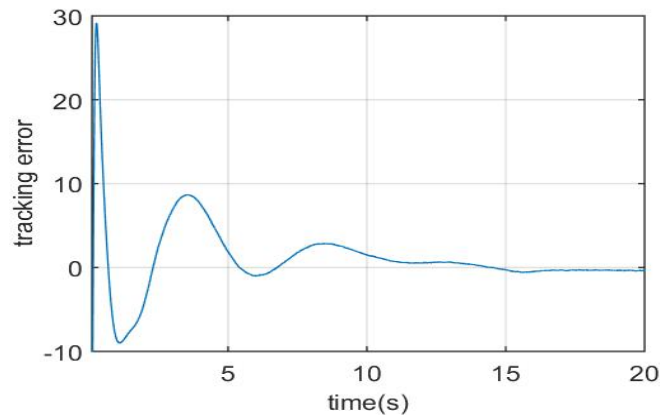**Fig. 11. A sample of nonlinear in-flight simulation of the guest aircraft response**

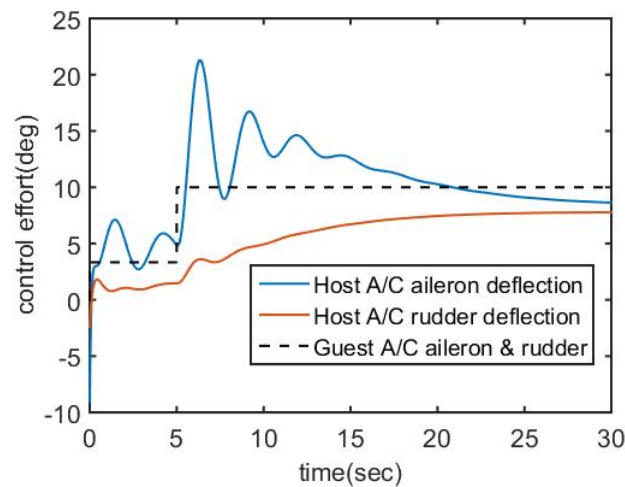**Fig. 12. The output tracking error in the longitudinal mode**

Fig. 13. A sample of aileron and rudder surface control input command for the of the guest aircraft against their equivalent control commands for the host aircraft
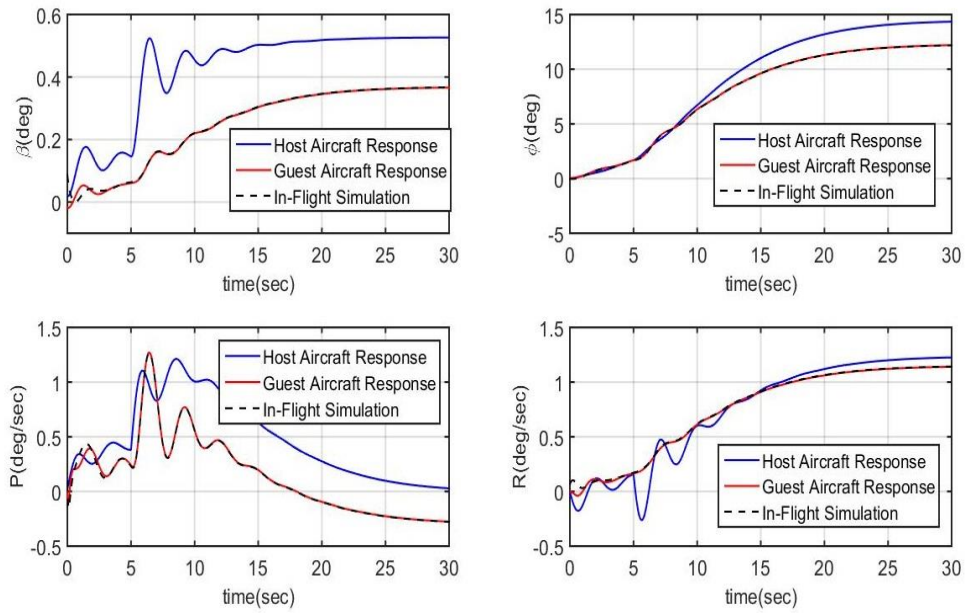
Fig. 14. a sample of nonlinear in-flight simulation of the guest aircraft response
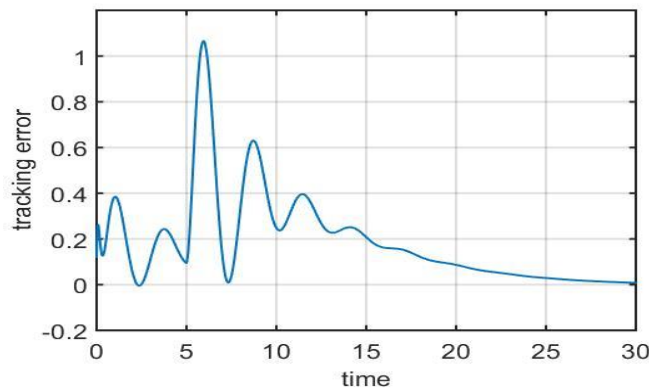

Fig. 15. The output tracking error in lateral mode

4.3 Validation of the results using the flight test data

In order to validate the capability of the designed controller for in-flight simulation and tracking the guest aircraft responses by the host aircraft simulator, the host aircraft simulates the flight test profile of the guest aircraft. For this reason, all the flight conditions of the guest aircraft at 2250s of the flight time, shown in Fig. 4, are derived in which they are considered as the initial conditions of the host aircraft simulator. Airspeed of 117 m/s, the altitude of 3580 m, pitch angle of -1.6 degrees, heading angle of 37 degrees and a zero roll angle are some of the initial conditions for the guest aircraft simulator. Then, the simulation is performed and the results of the in-flight simulation by the host aircraft simulator and the flight test of the guest aircraft are compared subsequently.

In this regard, Fig. 16 shows the comparison of the airspeed flight test of the guest aircraft versus its in-flight simulation by the host aircraft simulator. This figure demonstrates that the host aircraft model is capable of tracking the airspeed profile of the guest aircraft in the flight test data.

Fig. 17 illustrates the comparison of the guest aircraft altitude in the flight test versus its simulated altitude by the host aircraft simulator. A small bias in the flight test altitude tracking of the guest aircraft is found in this simulation. This bias is found because of a small difference between the initial flight test airspeed of the guest aircraft and the initial airspeed of the host aircraft simulator that is considered by the author to obviously illustrate the capability of the proposed controller. The host aircraft simulator requires a small drop of altitude in the initial times of the simulation to compensate its airspeed for tracking the reference airspeed signal of the guest aircraft.

Figs.18, 19 and 20 illustrate the comparison of the pitch, roll and heading angle in the flight test of the guest aircraft versus their in-flight simulation profile by the host aircraft simulator. As it is illustrated in the results, the flight simulator makes a perfect trajectory tracking during the simulation procedure.
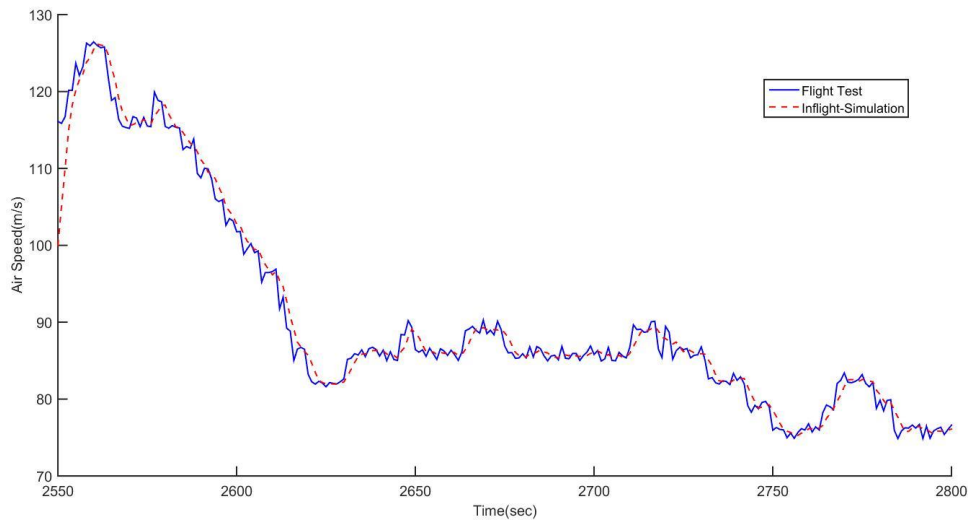
58

Fig. 16. The comparison of the airspeed flight test of the guest aircraft vs. its in-flight simulation by the host aircraft simulator
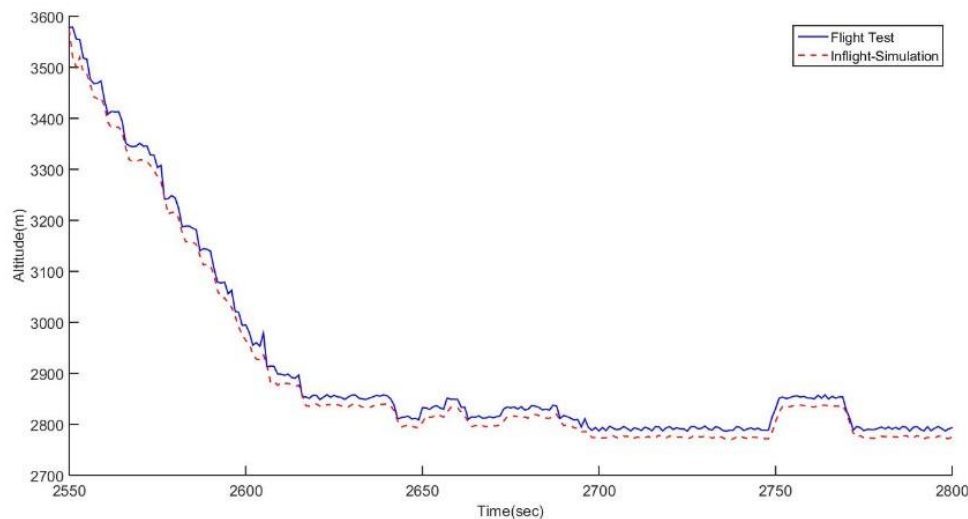

Fig. 17. The comparison of the aircraft altitude in the flight test of the guest aircraft vs. its in-flight simulation by the host aircraft simulator

The previous figures only present a sample of the guest aircraft trajectory tracking accomplished by the host aircraft simulator. In this regard, various flight test profiles for the guest aircraft are simulated and tracked by the host aircraft simulator and the results demonstrate a similar conclusion.

The comparison between the results of the flight test for the guest aircraft and its in-flight simulation profiles by the host aircraft simulator confirms that in-flight simulation of the guest aircraft dynamic by the host aircraft simulator is totally possible using the designed LQG controllers.

4.4 Comparing with other methods

This section describes the advantage of the proposed method in comparison with two other controllers. The first simple controller that could be used for in-flight simulation of the guest aircraft is the designed controller by the pole-placement method. It is obvious that this controller is only capable of changing the flight dynamic behavior of the host aircraft to simulate the dynamic behavior of the guest aircraft in the longitudinal and lateral modes. Hence, the pole-placement method adapts the properties of the short period, Phugoid, roll, Dutch-roll and spiral modes of the host aircraft to simulate the guest aircraft response. Therefore, this type of controller only simulates the modal properties of the guest aircraft while is incapable of tracking the flight profile for the guest aircraft and a perfect in-simulation of the guest aircraft responses cannot be achieved as well.

Mohammadi and Mortazavi [17] designed a controller, which uses the pole-placement and tracking methods to simulate the guest aircraft response by the host aircraft simulator. The strength of their applied method comparing by the pole-placement method is that in addition of changing the host aircraft dynamic behavior, it could track the flight profile of the guest aircraft. The weakness of their proposed method
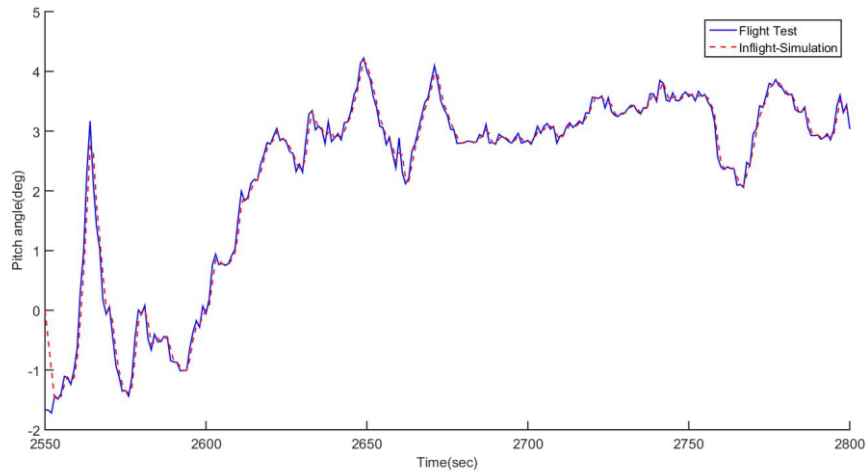
Fig. 18. The comparison of the pitch angle in the flight test of the guest aircraft vs. its in-flight simulation by the host aircraft simulator
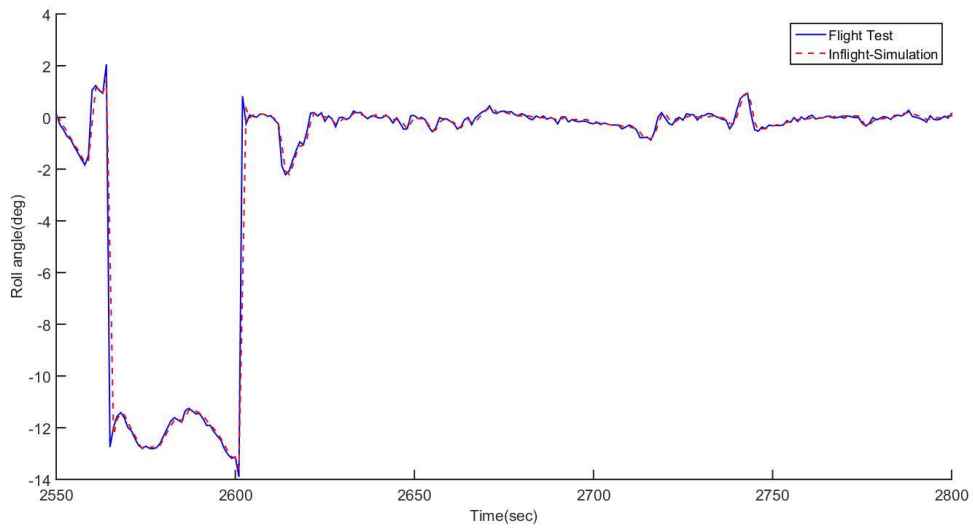

Fig. 19. The comparison of the roll angle in the flight test of the guest aircraft vs. its in-flight simulation by the host aircraft simulator
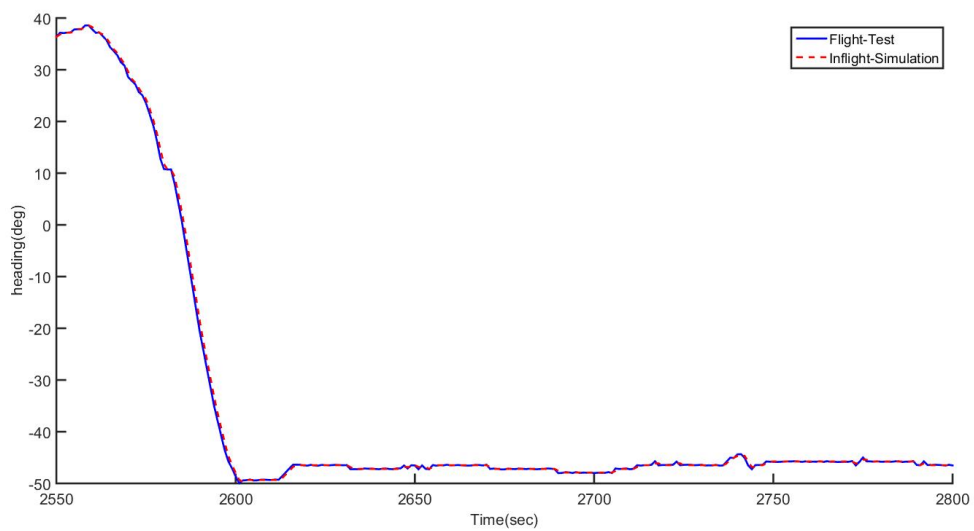

Fig. 20. The comparison of the heading in the flight test of the guest aircraft vs. its in-flight simulation by the host aircraft simulator

is that when the simulation starts, the tracking error during the flight simulation increases by the time and consequently a perfect and optimal tracking performance could not be achieved.

However, the strength of the proposed method is that while the dynamic behavior of the host aircraft is changing to simulate the guest aircraft dynamics, the flight profile of the guest aircraft can be perfectly tracked and the tracking error during the flight simulation reduces by the time.

5- CONCLUSION

In-flight simulation of a guest aircraft dynamic is performed and analyzed by a host aircraft simulator. in this paper, the LQG controllers are used to simulate the guest aircraft behavior by the host aircraft simulator.

The results demonstrated that the LQG controllers are capable of changing the host aircraft dynamics and simulate the guest aircraft response in the longitudinal and lateral modes.

The strength of the proposed method is that while the flight profile of the guest aircraft can be perfectly tracked, the tracking error during the flight simulation can be reduced by the time.

NOMENCLATURE

A,B,C,D,E	System matrices
b	Wing span
c	Mean aerodynamic chord
C_l, C_y, C_n	Lateral non-dimensional aerodynamic derivatives
$a_i, b_i, e_i, f_i, g_i, h_i$ $i = 1,2,...$	Aerodynamic coefficients
C_x, C_m, C_z	Longitudinal non-dimensional aerodynamic derivatives
$\{C_{L_0} C_{L_\alpha} \ \ C_{L_\beta} \ \ C_{L_{\alpha\beta}} \ \ C_{L_{\alpha^2}}$ $C_{L_{\alpha^2\beta}} \ C_{L_{\alpha^3}} C_{L_{\alpha^2\beta}} \ C_{L_q} \ C_{L_{q\alpha}} \ ...\}$	Lift coefficient derivatives
e_i	Tracking error
E	Expected value
g	Acceleration due to gravity
$I_{xx}, I_{yy}, I_{zz}, I_{xz}, I_{xy}$	Aircraft moments of inertia
J	Cost function
K	The controller gain
L	Iteration number
L	Kalman gain
M	Aircraft Mass
N	Normal distribution
p,q,r	Aircraft angular velocity components
$\bar{q}$	Dynamic pressure
Q	Notation for Variance
$Q_1(t)$	State weighting matrix
$Q_2(t)$	Control weighting matrix
Q_{xu}	Weighting matrix
R	Notation for Variance
R_0	Reference command
S	Wing area
T	Thrust
u	Control vector
u,v,w	Aircraft velocity components
V	Aircraft velocity
x	State vector
$\hat{x}$	Estimation of x
x_E, y_E, h	Aircraft navigational parameters
y	System output
z	Observation vector
$\tilde{z}_\xi$	computed response estimate
α	Angle of attack
$\delta_e, \delta_a, \delta_r$	Aircraft control surfaces deflections
δ_h	Horizontal tail deflection
δ_{th}	Aircraft throttle command
∇	Gradient operator
γ	Flight path angle
ρ	Air density

ν	Measurement noise
ω	Process disturbances
ξ	Vector of unknown parameters
Ψ, Θ, Φ	Euler angles

REFERENCES

[1] M. Lone, A. Cooke, Review of pilot models used in aircraft flight dynamics. Aerospace Science and Technology, 34 (2014) 55-74.

[2] P.A. Reynolds, Total In-Flight Simulator (TIFS)-A New Aircraft Design Tool, Journal of Aircraft, 9(6) (1972) 392-398.

[3] N.C. Weingarten, An In-Flight Investigation of Various Longitudinal Flight Control Systems in the Space Shuttle Orbiter during Approach and Landing, Technical Report 7263-1, Arvin/Calspan Advanced Technology Center, Buffalo, NY; Dec 1985.

[4] M. Malekzadeh, H. Sadeghian, Attitude control of spacecraft simulator without angular velocity measurement, Control Engineering Practice, 84 (2019) 72-81.

[5] N.C. Weingarten, In-Flight Simulation of the Space Shuttle Orbiter during Landing Approach and Touchdown in the Total In-Flight Simulator (TIFS), Technical Report 6339-F-1, Arvin/Calspan Advanced Technology Center, Buffalo, NY; Sep. 1978.

[6] M.F. Shafer, Inflight Simulation Studies at NASA Dryden Flight Research Facility, Dryden Flight Center. NASA Technical Memorandum 4396, Edwards, California, 1992.

[7] B.G. Powers, S.K. Sarrafian, Simulation Studies of Alternate Longitudinal Control Systems for the Space Shuttle Orbiter in the Landing Regime, In AIAA Atmospheric Flight Mechanics Conference Proceedings. Virginia: Williamsburg, Aug 1986, AIAA-86-2127, pp 182–192.

[8] K. Johansson, P. Dyreklev, O. Granbom, M.C. Calver, S. Fourtine, Feuillatre o. In-flight and ground testing of single event upset sensitivity in static RAMs, IEEE Transactions on Nuclear Science, 45(3) (1998) 1628-1632.

[9] D.T. Berry, B.G. Powers, K.J. Szalai, R.J. Wilson, In-Flight Evaluation of Control System Pure Time Delays, Journal of Aircraft, 19(4) (1982) 318–323.

[10] M. Sato, Gain-Scheduled Flight Controller Using Bounded Inexact Scheduling Parameters, IEEE Transactions on Control Systems Technology, 27(3) (2018) 1074-1082.

[11] M. Sato, A. Satoh, Flight Control Experiment of Multipurpose-Aviation-Laboratory-alpha In-Flight Simulator. Journal of Guidance, Control, and Dynamics, 34(4) (2011) 1081-1096.

[12] S. Corda, R.J. Franz, J.N. Blanton, M.J. Vachon, J.B. Deboer, In-Flight Vibration Environment of the NASA F-15B Flight Test Fixture. NASA/TM-2002-210719, NASA Dryden Flight Research Center, Edwards, California, February 2002.

[13] N.C. Weingarten, History of In-Flight Simulation & Flying Qualities Research at Calspan, Journal of Aircraft, 42(2) (2005) 1-16.

[14] C. Kim, A. Study on the Design and Validation of Switching Control Law, Journal of Institute of Control, Robotics and Systems, 17(1) (2011) 54-60.

[15] S. Fernandes, Guidance and Trajectory Following of an Autonomous Vision-Guided Micro Quadrotor, Lisbon, Portugal: Universidade Tecnica de Lisboa, 2011.

[16] A.A. Pashilkar, Trends in Simulation Technologies for Aircraft Design, Journal of Aerospace Science and Technology, 22(1) (2014) 1-10.

[17] S.J. Mohammadi, M. Mortazavi, Design of Tracking Controller for In-flight Simulation of Fighter Aircraft by UAV Platform, Mechanical Engineering Tabriz University, 47(3) (2017) 234-235.

[18] D.C. Watson, W.S. Hindson, In-flight simulation investigation of rotorcraft pitch-roll cross coupling, National Aeronautics and Space Administration, NASA, 2018.

[19] M.S. Chehadeh, Design of rules for in-flight non-parametric tuning of PID controllers for unmanned aerial vehicles, Journal of the Franklin Institute 356(1) (2019) 474-491

[20] B.L. Stevens, F.L. Lewis, Aircraft Control and Simulation, New York: John Wiley & Sons, 1992.

[21] J. Roskam, Airplane Flight Dynamics and Automatic Flight Control, Kansas: Lawrence University, 1979.

[22] R.C. Nelson, Flight Stability and Automatic Control, New York: McGraw-Hill, 1989.

[23] U. Ozdemir, M.S. Kavsaoglu, Linear and Nonlinear Simulation of Aircraft Dynamics Using Body Axis System, International Journal of aircraft engineering and aerospace technology, 80(6) (2008) 638-648.

[24] R.E. Maine, K.W. Iliff, Identification of Dynamic Systems-Applications to Aircraft. Part 1. The Output Error Approach, AGARD Flight Test Techniques-AG300, vol. 3, 1986.

[25] R.D. Grove, R.L. Bowles, S.C. Mayhew, A Procedure for Estimating Stability and Control Parameters from Flight Test Data by Using Maximum Likelihood Method Employing a Real Time Digital System, NASA TN D-6735, Washington, US; May 1972.

[26] M. Safi, M. Mortazavi, S. M. Dibaji, Global Stabilization of Attitude Dynamics: SDRE-based Control Designs, AUT Journal of Modeling and Simulation, 50(2) (2018) 203-210.

[27] L.W. Taylor, K.W. Iliff, System Identification Using a Modified Newton Raphson Method- A FORTRAN Program, NASA TN D-6734, Washington, US, May 1972.

[28] S. Skogestad, I. Postlethwaite, Multivariable Feedback Control-Analysis and Design, New York: John Wiley & Sons, 2005.

[29] J.L. Speyer, W.H. Chung, Stochastic Processes, Estimation, and Control (Advances in Design and Control), Los Angeles: Published by Society for Industrial Applied Mathematics, university of California, 2011.

[30] S. Hur, W.E. Leithead, Model predictive and linear quadratic Gaussian control of a wind turbine. Optimal Control, application, and methods, 38(1) (2017) 88-111.